


Quercetin suppresses ovariectomy-induced osteoporosis in rat mandibles by regulating autophagy and the NLRP3 pathway

Yue Xiong^{1*}, Cheng-Wei Huang^{2*}, Chao Shi³, Liang Peng³, Yu-Ting Cheng¹, Wei Hong³ and Jian Liao¹

¹Department of Prosthodontics and Implantology, School/Hospital of Stomatology, Guizhou Medical University, Guiyang 550004, P.R. China; ²AOSI CAR Dental, Shantou 515041, P.R. China; ³Guizhou Medical University, Guiyang 550004, P.R. China

*These authors contributed equally to this paper.

Corresponding authors: Jian Liao. Email: liaojian@gmc.edu.cn; Yue Xiong. Email: 510429863@qq.com

Impact Statement

Post-menopausal osteoporosis (PMOP) is a high prevalence in women in their 50s and it is also the age group of high demand for implant restoration. However, PMOP can affect bone mass and bone quantity, affecting the long-term success of implant restorations, and is a challenging clinical issue. Conventional treatment has some drawbacks and we attempted to find out if there was a possibility of using it clinically by comparing the effectiveness of the Chinese medicine quercetin (QR) with the traditional Western medicine alendronate (ALN) for bone quality improvement. We performed micro-computed tomography (micro-CT), western blotting, real-time quantitative PCR (RT-qPCR), pathological sections, and immunofluorescence experiments and showed that QR may restore bone quality and quantity by reducing osteoclast autophagy and the release of inflammatory factors from the NLRP3 pathway, with similar efficacy to ALN, which provides a promising outlook for the use of QR as a nutritional supplement for the prevention and treatment of PMOP.

Abstract

With the aging population and the popularity of implant prostheses, an increasing number of postmenopausal osteoporosis (PMOP) patients require implant restorations; however, poor bone condition affects the long-term stability of implant prostheses. This study aimed to investigate the therapeutic effect of quercetin (QR) compared with alendronate (ALN), the primary treatment for PMOP, on mandibular osteoporosis (OP) induced by ovariectomy (OVX) in female rats. Adult female rats were treated with QR (50 mg/kg/day), ALN (6.25 mg/kg/week) by gavage for 8 weeks, chloroquine (CQ, 10 mg/kg/twice a week), and cytokine release inhibitory drug 3 (MCC950, 10 mg/kg/three times a week) by intraperitoneal injection for 8 weeks after bilateral OVX. Blood samples were collected prior to euthanasia; the mandibles were harvested and subjected to micro-computed tomography (micro-CT) and pathological analysis. QR administration controlled weight gain and significantly improved the bone microstructure in OVX rats, increasing bone mass, and bone mineral density (BMD), reducing bone trabecular spacing, and decreasing osteoclast numbers. Western blotting, real-time quantitative PCR (RT-qPCR), and serum markers confirmed that QR inhibited interleukin-1 β (IL-1 β) and interleukin-18 (IL-18) on the nucleotide-binding oligomerization domain (NOD)-like receptor (NLR) protein 3 (NLRP3) pathway thereby inhibiting osteoclast differentiation, immunofluorescence and western blotting also confirmed that QR inhibited autophagy in OVX rats and suppressed the number of tartrate-resistant acid phosphatase (TRAP)-stained positive osteoclasts. The findings suggest that QR may protect the bone structure and prevent bone loss in osteoporotic rats by inhibiting the NLRP3 pathway and autophagy in osteoclasts with comparable

effects to ALN, thus QR may have the potential to be a promising alternative supplement for the preventive and therapeutic treatment of PMOP.

Keywords: Quercetin, alendronate, postmenopausal osteoporosis, autophagy, NLRP3, osteoclasts

Experimental Biology and Medicine 2024; 248: 2363–2380. DOI: 10.1177/15353702231211977

Introduction

Osteoporosis (OP) is a widespread, systemic, metabolic bone disease marked by a decrease in bone mineral density (BMD) and destruction of bone structure, in addition to a substantial increase in bone fragility and fracture susceptibility,¹ caused by an imbalance between bone resorption by osteoclasts and bone deposition by osteoblasts.^{1,2}

According to World Health Organization (WHO), about 200 million people worldwide are suffering from OP, and its incidence has jumped to the seventh place of common diseases among the elderly. In 2018, the National Health Council of China released the results of an epidemiological survey on OP, which showed that the prevalence of OP in people over 50 years of age was 19.2%, and the percentage of the low bone mass group was as high as 46.4%. Postmenopausal

women are at high risk for a disorder known as postmenopausal osteoporosis (PMOP), which is the most common type of OP and is mainly associated with decreased estrogen levels.³ A significant proportion of PMOP patients also suffer from dental defects, and they have a high demand for oral implant restorations. However, OP can easily lead to insufficient bone quantity and unhealthy bone quality decreased initial stability of implant placement, prolonged bone healing time, and weakened regeneration ability of the peri-implant bone, and changes in the local peri-implant bone microenvironment due to trauma and infection after implantation, which affect the success rate of implant surgery.⁴ With the development of society and aging, the incidence of PMOP is increasing annually. It seriously affects the quality of life of patients and brings a heavy economic burden to society, and has become a public health problem that needs to be solved worldwide. Moreover, methods to improve OP in postmenopausal women, increase the rate of implant osseointegration, and shorten the healing time have been the focus of research in oral implantology.

Autophagy is involved in the vital activities of osteoblasts, osteoclasts, and osteocytes,⁵ maintaining the dynamic balance between osteoblasts and osteoclasts in the physiological state and the stress response in the pathological conditions,^{6,7} and is closely related to bone loss diseases such as OP, playing an essential role in regulating bone homeostasis in the bone immune system.^{8,9} Nucleotide-binding oligomerization domain (NOD)-like receptor (NLR) protein 3 (NLRP3) inflammatory vesicles, as the body's first line of defense against pathogens, also play an active role in the pathogenesis of OP by inhibiting bone formation while promoting bone resorption, ultimately leading to bone loss.^{8,10,11} Studies have reported that NLRP3 inflammatory vesicles interact with autophagy to maintain the dynamic homeostasis of the body under stressful conditions. Autophagy removes damaged proteins and enriched organelles and disrupts intracellular pathogen-induced inflammatory response process. If autophagy is dysfunctional, it may lead to hyperactivation of NLRP3 inflammatory vesicles.¹²

Conventional treatment protocols for PMOP include bone resorption inhibitors (e.g. bisphosphonates, hormone replacement therapy, selective estrogen receptor modulators, and anti-RANKL (receptor activator of nuclear factor kappa B (NF- κ B) ligand) antibodies, and synthetic drugs (e.g. intermittent low-dose teriparatide and anti-sclerostin antibodies); however, these treatments are also associated with some adverse effects.^{13–15} Alendronate (ALN) is a third-generation amino diphosphonate bone resorption inhibitor with a strong affinity for intraosseous hydroxyapatite, which exerts an anti-resorptive effect by inhibiting osteoclast activity and has been commonly used in the treatment of PMOP. It is well tolerated with gastrointestinal reactions such as nausea, abdominal distension, abdominal pain, occasional headache, skeletal muscle pain, and rare rash or erythema. However, with the widespread use of this drug, the number of esophageal adverse events has increased, and side effects such as esophageal erosion and esophageal ulceration have occurred.¹⁶ Are there natural compounds with potent osteo-protective properties and fewer side effects that can be alternatives to overcome the shortcomings of existing therapies?

Quercetin (C₁₅H₁₀O₇; QR) is the major monomer component of eucommia flavonoid subclasses, widely exists in plants in nature, and is a naturally occurring acute coenzyme transport inhibitor.¹⁷ The keto carbonyl group can generate basic oxygen atoms of strongly acidic salts, and the presence of phenolic hydroxyl groups and their double bonds also enhances the antioxidant effect of QR. These molecular structures make it significant in the effective scavenging of free radicals in the body, maintaining the normal structure and function of body cells, preventing tumor mutations, and delaying the onset of aging.¹⁸ QR has been shown to have estrogen-like effects and promote osteogenesis by inhibiting bone resorption and having an anti-osteoporotic effect.¹⁹ The addition of 0.25% QR to the diet of rats with ovaries removed was able to slow down bone resorption, and particularly to inhibit bone loss due to estradiol deficiency.²⁰

Does QR exert a therapeutic effect on OP by regulating autophagy and inhibiting the NLRP3 inflammasome? However, this has not been reported yet. As QR has been used as a health supplement for many years and has potent antioxidant, anti-inflammatory, and autophagy-promoting effects, we hypothesized that QR might be a promising, multi-targeted inhibitor of osteoclast activation, making alveolar bone free from osteoclast/inflammation-mediated bone resorption. This study investigated the anti-osteoporotic effect of QR in a bilateral ovariectomy (OVX)-induced PMOP rat model, with the aim of comparing its efficacy with that of ALN, the main therapeutic agent for PMOP.

Materials and methods

Chemicals

QR (10.0 g, purity \geq 95%) was purchased from Sigma Chemical company (CAS No.: 117-39-5). ALN Tablets (Fosamax; Specification: 70 mg/tablet), Production Lot No.: J20170085, Merck Sharp & Dohme, Inc. Chloroquine (CQ), an autophagy inhibitor (specification: 1.0 g; purity: 97%), was purchased from Shanghai Macklin Biochemical company (CAS No.: 54-05-7); NLRP3 pathway inhibitor CRID-3, Cytokine release inhibitory drug 3 (MCC950, specification: 2.0 g; purity \geq 98%), was purchased from Sichuan Weikeqi Biological Technology company (CAS No.: 256373-96-3). Propeptide of type I procollagen (PINP), cross-linked C-telopeptide of type 1 collagen (CTX-1), interleukin-1 β (IL-1 β) and interleukin-18 (IL-18) enzyme-linked immunosorbent assay (ELISA) kits were purchased from Quanzhou Ruixin Biotech company. Hematoxylin-eosin (HE), and tartrate-resistant acid phosphatase (TRAP) staining kits were purchased from Beijing Solarbio Science and Technology company. Antibodies against caspase-1 (#24232), IL-1 β (#12507), and NLRP3 (#15101) were purchased from Cell Signaling Technology (CST) company. Antibodies against LC3 (14600-1-AP), Beclin1 (11306-1-AP), and p62 (18420-1-AP) were purchased from Proteintech company. Antibodies against β -actin (ab8226), IL-18 (ab191860) were purchased from Abcam company. Goat anti-rabbit IgG (E-AB-1003) was purchased from Elab Science company. Cy3 conjugated Goat Anti-Rabbit IgG (H + L) (GB21303) was purchased from Servicebio company.

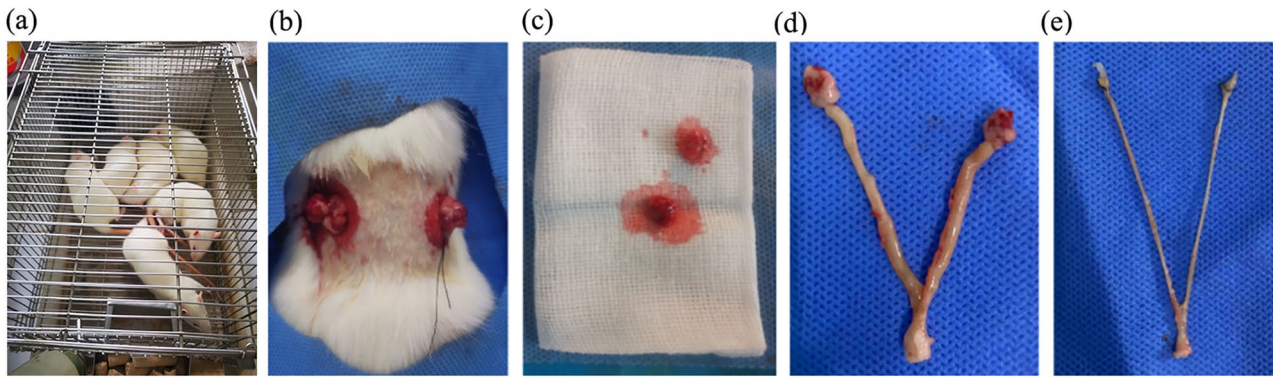


Figure 1. (a) 12-week-old SD rats, (b) ligation of both ovaries, (c) removed bilateral ovaries, (d) uterine morphology of rats in SHAM group after 12 weeks, and (e) uterine morphology of rats in the OVX group 12 weeks after OVX.

Animals

Ninety-six adult female Sprague-Dawley (SD) rats were used in this study. These animals were housed in a 12-h alternating light/dark cycle. Rodent standard feed and water were provided ad libitum. The rats were randomized into eight different groups, including: group 1: sham operation (SHAM); group 2: ovariectomy (OVX); group 3: ovariectomy + 50 mg/kg/day QR (OVX + QR); group 4: ovariectomy + 6.25 mg/kg/week ALN (OVX + ALN); group 5: ovariectomy + 10 mg/kg/twice a week chloroquine (OVX + CQ); group 6: ovariectomy + 10 mg/kg/twice a week chloroquine + 50 mg/kg/day QR (OVX + CQ + QR); Group 7: ovariectomy + 10 mg/kg/three times a week MCC950 (OVX + M); Group 8: ovariectomy + 10 mg/kg/three times a week MCC950 + 50 mg/kg/day QR (OVX + M + QR). All QR and ALN treatments were administered by gavage, with equal volumes of saline in the SHAM and OVX group, whereas CQ and MCC950 were administered by intraperitoneal injection. All treatments were started at 12 weeks after the OVX and lasted for 8 weeks. The doses and durations of QR, CQ, and MCC950 were selected based on previous studies.^{21–23} Dosage calculation of ALN is based on the body surface area calculation method. All experimental procedures were approved by the Ethics Committee for Animal Experiments of Guizhou Medical University on January 10, 2022 (approval number: 2201633), with Yue Xiong using the animals under a protocol that had been approved (SCXK; 2018-0001). The National Institute of Health of the United States and the International Council on Research Animal Care's "Guide for the Care and Use of Laboratory Animals" were followed during all experimental procedures.

OVX procedure

After fasting and water fasting for 12 h, the 12-week-old rats were anesthetized by intraperitoneal injection of 3% pentobarbital sodium (35 mg/kg) and fixed on a surgical plate. Bilateral OVX was performed using the dorsal method, wherein the dorsal side of the animal was shaved and sterilized with 75% ethanol. A 1-cm-long incision was made under aseptic conditions, and both ovaries were ligated and removed. The incision was closed in layers, and lidocaine and penicillin powder were applied locally to the incision

area. The SHAM group removed equal volumes of adipose tissue adjacent to the ovaries. The model was established 12 weeks after ovarian removal. The results showed that the uterus of SD rats in the OVX group was atrophied and the morphology differed significantly from that of the SHAM group, suggesting successful modeling (see Figure 1).

Sample collection

The body weights of the rats were measured one day after OVX and before the start of weekly treatment. After 8 consecutive weeks of treatment, blood samples were collected from the abdominal aorta after anesthetizing the rats with an intraperitoneal injection of 3% sodium pentobarbital (35 mg/kg), and the serum obtained was subjected to biochemical analysis under appropriate storage conditions before euthanasia of the rats by increasing the anesthetic dose. The mandibles of each rat were removed and cleaned of cartilage, adherent tissue, and bone marrow, and then the mandibles were divided into the right and left sides. One side of the mandible was stored at -80°C for real-time quantitative PCR (RT-qPCR), and western blot assay, and the other side of the mandible was partially stored in electron microscopy fixative, decalcified, embedded, sectioned, and used for transmission electron microscopy, and partially stored in 4% paraformaldehyde, undecalcified for micro-computed tomography (micro-CT) scanning and analysis. The remaining mandibles were decalcified using 10% ethylene diamine tetraacetic acid (EDTA) decalcification solution for approximately 4 weeks until a 10 mL syringe needle could be easily inserted, dehydrated in ethanol step by step, waxed, paraffin-embedded, sectioned (5 μm), and used for staining, and immunofluorescence.

Micro-CT scan and analysis of rat mandible

After completion of calibration, the undecalcified unilateral mandible was taken and placed in 10% neutral buffered formalin seeds for 24 h of fixation, and excess soft tissue was removed. The mandible was scanned using a Skyscan 1276 micro-CT instrument (Bruker micro-CT Kontich, Belgium) with the following scan settings: source voltage, 70 kV; source current, 200 μA ; Al 0.5 mm filter; pixel size 6 μm ; and rotation step of 0.3 degrees. Images were constructed with

Table 1. Primer sequences.

Primer	Primer sequence	Length of product (bp)
GAPDH	(S) 5'-CTGGAGAAACCTGCCAAGTATG-3' (A) 5'-GGTGAAGAATGGGAGTTGCT-3	138
caspase-1	(S) 5'-TGCCTGGTCTTGTGACTTGGAG-3' (A) 5'-TGTCTGGGAGAGGTAGAAACG-3	132
NLRP3	(S) 5'-GATTCTCCACAACCTACCCAA-3' (A) 5'-AGTCTGGAAGAACAGGCAACAT-3	112

NLRP3: nucleotide-binding oligomerization domain (NOD)-like receptor (NLR) protein 3; GAPDH: glyceraldehyde-3-phosphate dehydrogenase.

NR econ software (Bruker micro-CT, Kontich, Belgium) with the following settings: ring artifact correction: 3; smoothing: 3; and beam hardening correction: 30%. The interradicular septum extending from the furcation roof to the root apices of the first molar was selected as the region of interest (ROI). The following parameters were measured: bone volume fraction (BV/TV), bone trabecular number (Tb. N), bone trabecular thickness (Tb. Th), bone trabecular separation (Tb. Sp), and BMD. All data were analyzed using the CTAn program (Bruker micro-CT, Kontich, Belgium).

Detection of serum bone metabolism indexes

Three months after modeling and 8 weeks after drug intervention, rats in each group were anesthetized with 3% sodium pentobarbital 35 mg/kg intraperitoneally, and 3–5 mL of blood was collected from the abdominal aorta, centrifuged at 3000 revolutions per minute (RPM) for 15 min at 4°C, and the serum was extracted and stored in a refrigerator at –80°C. The serum levels of IL-18, IL-1β, PINP, and CTX-1 in the serum were determined according to the standards of the ELISA kit.

RT-qPCR to measure the expression of caspase-1 and NLRP3 mRNA

The mandibles of rats in each group stored at –80°C were obtained. The cancellous bone of the jaw was then collected, ground into powder, and the total RNA was extracted using the triazole technique. RNA concentration and purity were then determined using a Nanodrop 2000 reaction system: 2 × SYBR Premix Ex Taq II 7.5 μL, upstream and downstream primers 1.5 μL, cDNA: 2 μL, plus dH₂O 4.0 μL; 95°C –30 s; 95°C –15 s, 60°C –30 s, 40 cycles; melting curve: fluorescence signals were collected at each 0.5°C rise in temperature from 65°C to 95°C. With the primer sequences listed in Table 1, the expressions of the *caspase-1* and *NLRP3* genes were assessed. Glyceraldehyde-3-phosphate dehydrogenase (GAPDH) mRNA levels served as the baseline for the other mRNA levels. Relative gene expression levels were calculated using the 2^{–ΔΔCt} technique.

Western blot detection of NLRP3 pathway and autophagy-related protein expression in rat mandibular bone tissue

Weighed 50–100 mg of frozen mandibular bone tissue specimens were taken and ground in liquid nitrogen, and then put into 1.5 mL EP tubes, 200 μL radio immunoprecipitation assay

(RIPA) lysis solution containing protease inhibitor was added to each tube, lysed on ice for 40 min, centrifuged at 4°C for 25 min at 12,000 RPM, the supernatant was obtained, and the total protein from bone tissue was extracted. Bicinchoninic Acid (BCA) Protein Quantification Kit was used to quantify the proteins, which were subjected to SDS-polyacrylamide gel electrophoresis (PAGE), membrane transfer, and overnight incubation at 4°C with 1:1000 diluted IL-1β, IL-18, caspase1, NLRP3, LC3, Beclin1, and 1:5000 diluted p62 and β-actin antibodies. Horseradish peroxidase-labeled goat anti-rabbit IgG (1:5000) was added, incubated for 2 h at room temperature, and photographed after color development with ECL color development kit. The protein expression levels were determined by analyzing the grayscale values with β-actin as the reference, and three replicates were set for each group.

Immunofluorescence assay

Immunofluorescence technique was used to assess the expression of LC3 and Beclin1 proteins. After rehydration in a warmed alcohol and phosphate-buffered saline (PBS), the alcohol series and PBS were permeabilized. Permeabilization was performed with 0.3% Triton X-100 for 30 min at room temperature. Sections were then blocked with 10% goat serum in PBS for 30 min. Sections were incubated with the primary monoclonal antibodies to LC3 (14600-1-AP, Servicebio at dilution of 1:500 in PBS), Beclin1 (11306-1-AP, at dilution of 1:50 in PBS), and p62(18420-1-AP, at dilution of 1:1500 in PBS) overnight, followed by conjugation with a secondary polyclonal antibody Cy3 conjugated Goat Anti-Rabbit IgG (H + L) at 37°C (GB21303, 1:200 in PBS) for 1.5 h. After rinsing with PBS four times, the sections were incubated with 4',6-diamidino-2-phenylindole (DAPI). The sections was incubated with DAPI for 5 min and observed under a fluorescence microscope. Images were captured at ×200 magnification fluorescence microscopy (Olympus BX51) equipped with an Olympus DP70 digital camera. Immunofluorescence staining was quantified using ImageJ software (version 1.37; National Institutes of Health, USA). For this purpose, five different microscopic areas were randomly investigated by a blinded investigator using fluorescence microscopy.

Histopathological changes of rat mandibles observed by HE and TRAP staining

Each group of decalcified, embedded, and sectioned rats had their alveolar bone dyed under the directions of the HE and TRAP staining kits before being observed under a light microscope and photographed.

Statistical analysis

Statistical analysis was performed using SPSS22.0 software (IBM Corp., Armonk, NY, USA), and statistical graphs were drawn using GraphPad Prism 9.5. Measurement data were expressed as mean and standard deviation (SD) when they were tested to be normally distributed. Comparisons between two groups were performed using the *t*-test or rank sum test, and multiple group comparisons were made by analysis of variance (ANOVA, one-way ANOVA and two-way ANOVA). If the measure data did not satisfy normal distribution, the Kruskal-Wallis test was used instead.

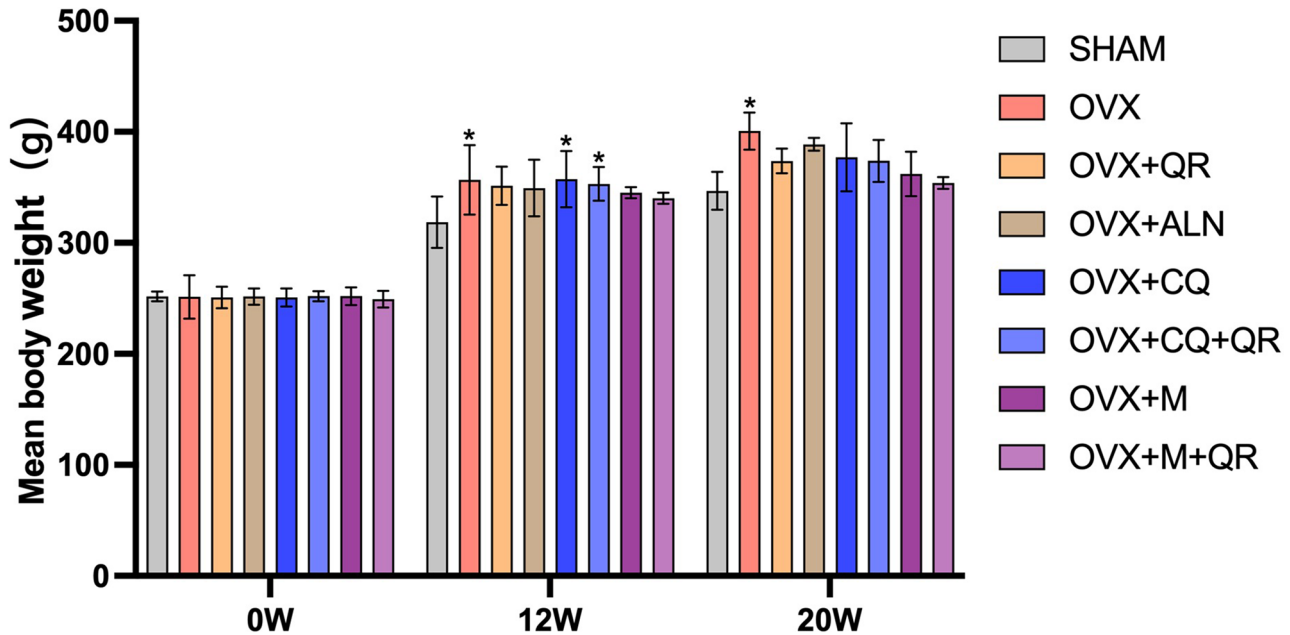


Figure 2. Mean body weights of rats.

Data are expressed as mean (SD) of $n=10$ from three independent measurements.

SD: standard deviation; SHAM: sham-operated group; OVX: ovariectomy; QR: quercetin; CQ: chloroquine; M: MCC950.

* $P < 0.05$ was considered statistically significant compared with SHAM group.

The test level was $\alpha = 0.05$, and $P \leq 0.05$, which was considered statistically significant.

Results

Effect of OVX and treatment on changes in body weight of rats

The mean body weight of rats increased significantly with longer rearing time after the removal of bilateral ovaries, with statistically significant differences ($P < 0.05$). At the fifth month after surgery, the body weight of rats in the OVX group was significantly greater than that of the SHAM group, while treatment with QR, ALN, CQ, and MCC950 controlled the body weight of rats, with no statistical difference compared to the SHAM group. There were no statistically significant differences in the effects of QR alone, or in combination with CQ or MCC950, on rat body weight (see Figure 2).

Effect of OVX and treatment on mandibular bone and bone trabecular parameters

In the left mandibular first molar apical compartment alveolar bone area, after 8 weeks of treatment, bone trabeculae in the mandibular alveolar bone were dense and well aligned in the SHAM group. In the OVX group, bone volume was lost, bone trabeculae became thin and narrow, and the degree of dispersion between trabecular bone increased. After treatment with QR and ALN, bone volume was restored and an increase in the number of bone trabeculae was observed, bone trabeculae were dense and well aligned, and the degree of separation was significantly reduced (see Figure 3(a) and (b)).

Bone microstructural parameters of the alveolar bone were derived from the analysis of the ROI region by micro-CT scanning. After 8 weeks of treatment, BV/TV, Tb. Th, and

BMD decreased and Tb. Sp increased in the OVX group of rats compared to the SHAM group, with all differences being statistically significant ($P < 0.05$) except for Tb. Th, indicating successful modeling of the OP model. Compared with the OVX group, the QR and ALN groups showed increased BV/TV, BMD, and Tb. N, decreased Tb. Sp ($P < 0.05$), but there was no significant difference in Tb. Th ($P > 0.05$); no significant difference was observed between these two treatment groups ($P > 0.05$; see Figure 3(c) to (g)).

Effect of OVX and treatment on serum biochemical markers of bone metabolism

After 8 weeks of treatment, the bone resorption index CTX-1 and bone formation index PINP were both increased to different degrees in the OVX group compared with the SHAM group, indicating that the rate of bone conversion was higher in the OVX rats and the bone tissue was in a highly reconstructed state. However, both bone conversion indices decreased to varying degrees when subjected to the effects of QR, ALN, M, or CQ, indicating that the bone tissue reconstruction became stable. There was no significant difference between the treated group and the SHAM group, but there was a statistically significant difference compared to the OVX group. CQ administered alone decreased PINP, but there was no statistically significant difference compared with the OVX group; when combined with QR, PINP significantly decreased ($P < 0.05$), suggesting that QR may have a synergistic effect with CQ. As for CTX-1, there was no significant difference in the reduction effect of CQ used alone or in combination with QR (see Figure 4(a) and (b)). M either alone or in combination with QR displayed favorable effect in reducing PINP and CTX-1.

Following 8 weeks of treatment, the serum levels of IL-1 β and IL-18 increased to different degrees in the OVX

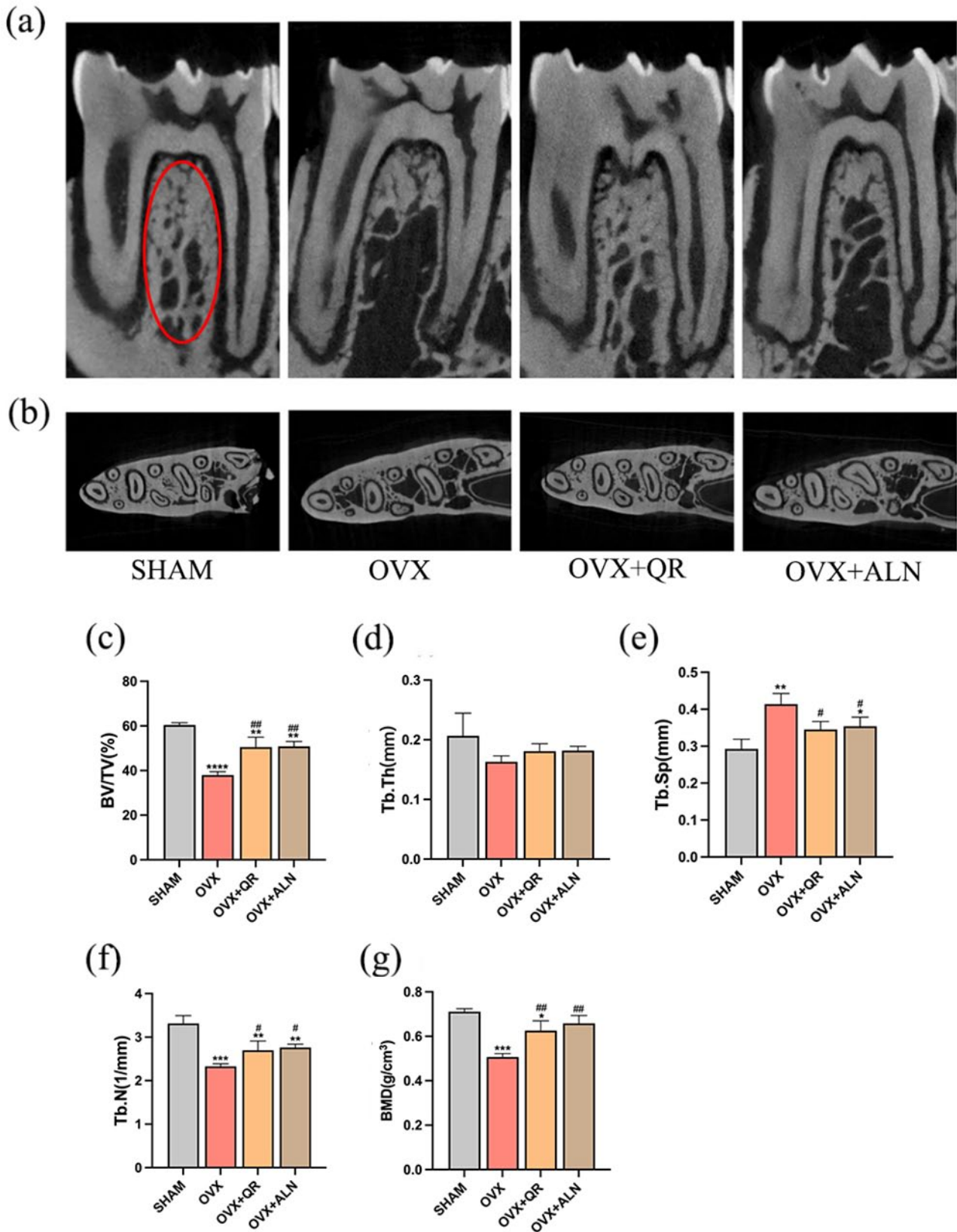


Figure 3. Micro-CT images of rat mandibular alveolar bone. (a) Sagittal plane of rat mandibular first molar, (b) cross-section of rat mandibular first molar. Bone microstructural parameters of the alveolar bone as (c) bone volume fraction (BV/TV), (d) bone trabecular thickness (Tb. Th), (e) bone trabecular separation (Tb. Sp), (f) trabecular number (Tb. N), and (g) bone mineral density (BMD) were derived from the analysis of the red circle area, which is the region of interest (ROI) by micro-CT scanning. Data are expressed as mean (SD) of $n=3$ from three independent measurements. * $P < 0.05$, ** $P < 0.01$, *** $P < 0.001$, **** $P < 0.0001$, all compared with SHAM group. # $P < 0.05$, ## $P < 0.01$, all compared with OVX group.

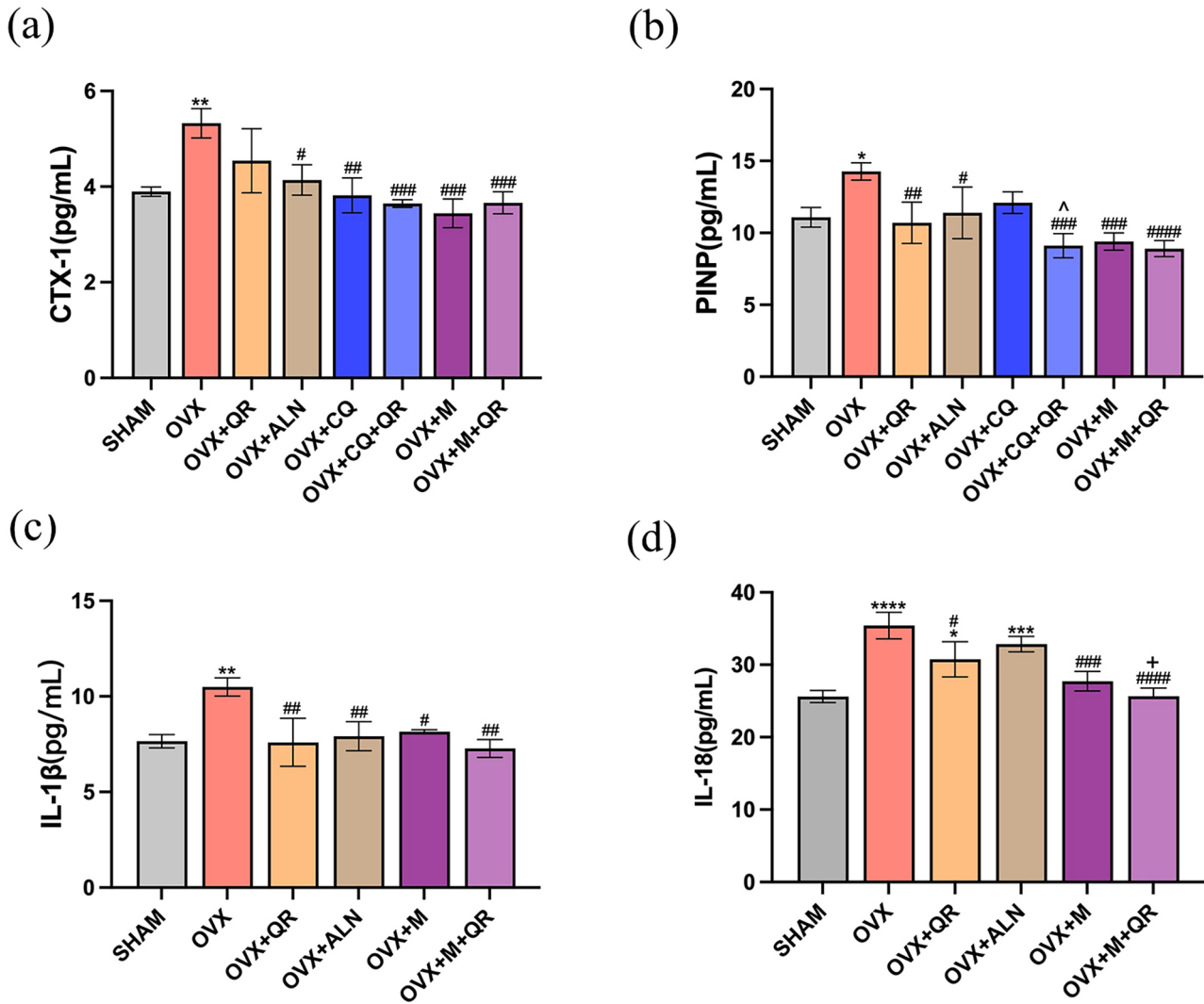


Figure 4. Effect of OVX and treatment on serum biochemical markers of bone metabolism. Variations in the serum levels of (a) CTX-1, a marker of bone resorption and (b) PINP, a marker of bone growth. Serum levels of (c) IL-1 β and (d) IL-18 in rats in each group.

Data are expressed as mean (SD) of $n=6$ from three independent measurements.

* $P < 0.05$, ** $P < 0.01$, *** $P < 0.001$, **** $P < 0.0001$, all compared with SHAM group.

$P < 0.05$, ## $P < 0.01$, ### $P < 0.001$, #### $P < 0.0001$, all compared with OVX group.

^ $P < 0.05$ compared with OVX + CQ group.

+ $P < 0.05$ compared with OVX + QR group.

group compared to the SHAM group ($P < 0.05$), indicating that inflammatory factors increased in the serum of rats after ovarian removal. However, the levels of inflammatory factors IL-1 β and IL-18 decreased to different degrees after treatment with QR, ALN, M, or Except for the IL-18 reduction after ALN treatment ($P > 0.05$), the rest of the treatment groups were statistically different compared to the OVX group ($P < 0.05$). IL-18 was significantly reduced by M in combination with QR, than by QR alone ($P < 0.05$). For IL-1 β , the effect of M in conjunction with QR was similar to the effect of both used individually (Figure 4(c) and (d)).

Effect of OVX and treatment on mRNA levels of NLRP3 signaling pathway-related genes in rat mandibular alveolar bone tissue

RT-qPCR results revealed that *caspace-1* and *NLRP3*, two genes connected to the NLRP3 signaling pathway, had

significantly higher levels of expression in the osteoporotic state of alveolar bone tissue than in the SHAM group ($P < 0.05$). Comparatively, caspase-1 and NLRP3 expression levels decreased after treatment with QR and ALN, with caspase-1 decreasing more significantly ($P < 0.05$). Caspase-1 and NLRP3 responses to the NLRP3 pathway inhibitor MCC950 alone or in combination with QR did not differ noticeably (see Figure 5).

Effect of OVX and treatment on the expression of NLRP3 pathway-related proteins as well as autophagy-related proteins

Compared to the SHAM group, NLRP3, caspase-1, IL-1 β , IL-18, Beclin1 protein expression, and LC3II/I ($P < 0.05$), and p62 protein expression ($P > 0.05$) were upregulated in the OVX group at the same time point of 8 weeks of treatment. The expression levels of NLRP3, caspase-1, IL-1 β , IL-18, and Beclin1 were lower in the QR and ALN groups than in the

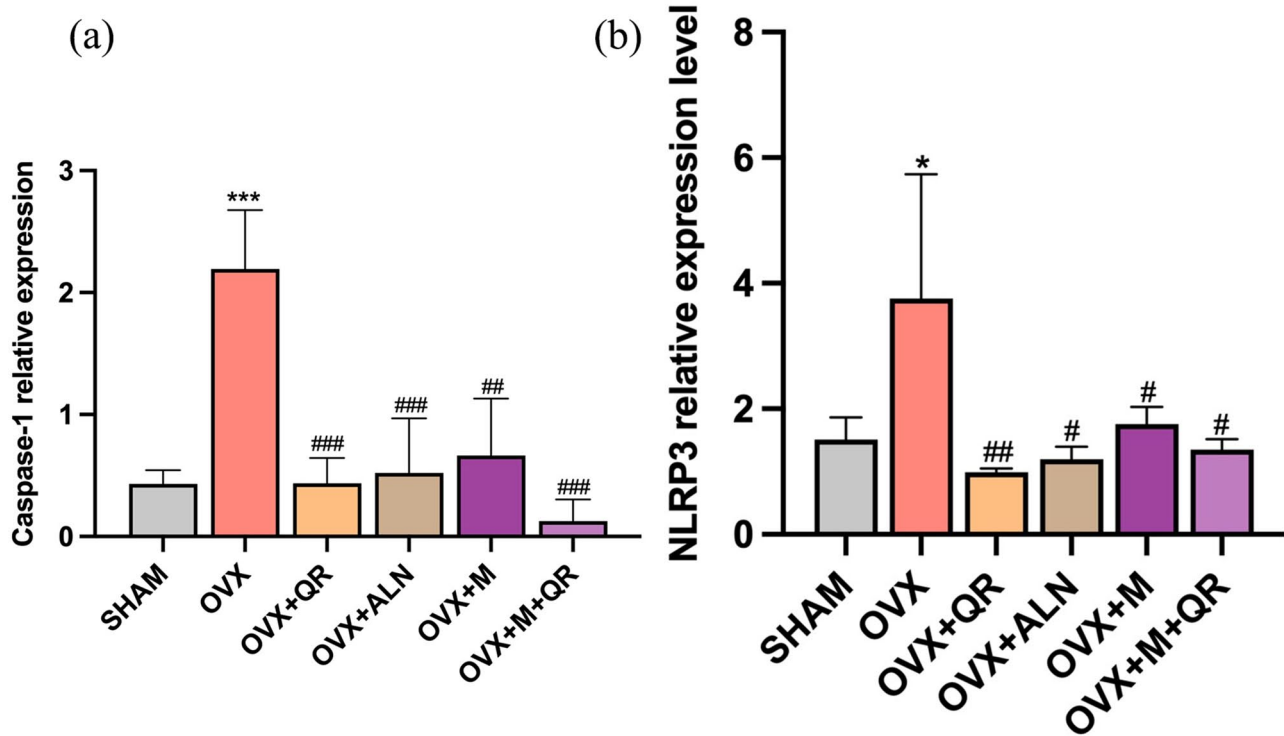


Figure 5. Effect of OVX and treatment on mRNA levels of NLRP3 signaling pathway-related genes as (a) *caspase-1* and (b) *NLRP3* in rat mandibular alveolar bone tissue.

Data are expressed as mean (SD) of $n=6$ from three independent experiments.

*** $P < 0.001$ compared with SHAM group.

$P < 0.01$, ### $P < 0.001$, all compared with OVX group.

OVX group ($P < 0.05$), while the expression levels of IL-1 β , Beclin1, and LC3II/I were not significantly different in the SHAM group compared to the QR group. ALN reduced caspase-1 more effectively than QR did, with no significant differences in the remaining indicators (see Figure 6).

In comparison to the SHAM group, Beclin1 ($P < 0.05$), and p62 ($P > 0.05$) protein expression and LC3II/I ($P < 0.05$) were upregulated in the OVX group at the same time point at 8 weeks. Compared to the OVX group, Beclin1 protein expression levels and LC3II/I were decreased ($P < 0.05$) in the QR, CQ, and CQ + QR groups; QR, and CQ had similar effects on Beclin1 and LC3II/LC3I; whereas p62 protein expression increased only statistically differently with CQ alone or in combination with QR. The combination of CQ and QR had a more noticeable effect on Beclin1 reduction ($P < 0.05$), whereas the effects on LC3II/I and p62, were not significantly different (see Figure 7(a)).

The protein expression of NLRP3, caspase-1, IL-1 β , and IL-18 was upregulated in the OVX group compared with the SHAM group at the same time point at 8 weeks ($P < 0.05$), while the expression levels of NLRP3, caspase-1, IL-1 β and IL-18 protein were all reduced in the QR, M, and M + QR groups when compared to the OVX group ($P < 0.05$). The use of M was more significantly effective than the use of QR in reducing NLRP3, whereas for the other three proteins, QR was able to achieve similar inhibitory effects as M. The combined use of M and QR was more effective in lowering NLRP3 and caspase-1 levels than either treatment alone, but was less effective in reducing IL-1 β and IL-18 levels (see Figure 7(b)).

Immunofluorescence

Immunofluorescence staining (see Figure 8) revealed red-fluorescent Beclin1, LC3, and p62-positive cells within the mandibular region of OVX rats, with blue-fluorescent nuclei in all cells. When the images were merged, the red and blue fluorescence overlapped, and the red fluorescence was mostly located in the osteochondral cancellous region of the rat mandible. In the SHAM group, red fluorescence was occasionally observed in Beclin1, LC3, and p62 positive cells, while in the OVX group, the intensity of Beclin1 and LC3 red fluorescence was significantly higher ($P < 0.05$) and the average fluorescence of p62 was comparable to that of SHAM. After treatment with QR, CQ, or a combination of both, Beclin1 and LC3 fluorescence intensity significantly decreased ($P < 0.05$), and p62 fluorescence intensity increased ($P < 0.05$), indicating that QR inhibited Beclin1 and LC3 expression and promoted p62 accumulation in the mandibular alveolar bone of OVX rats, with no significant difference from the effect of CQ alone or in combination ($P > 0.05$).

Effects of QR on histopathological changes in the mandibular alveolar bone of OVX rats

HE staining showed that the alveolar bone trabeculae in the SHAM group were more continuous, neatly arranged, morphologically intact, and without significant pathological changes. In the OVX group, the alveolar bone trabeculae were thinner and narrower, discontinuous, with more free ends, and the bone marrow cavity was widened, with a large number of osteoclasts and vacuolated fat cells, and

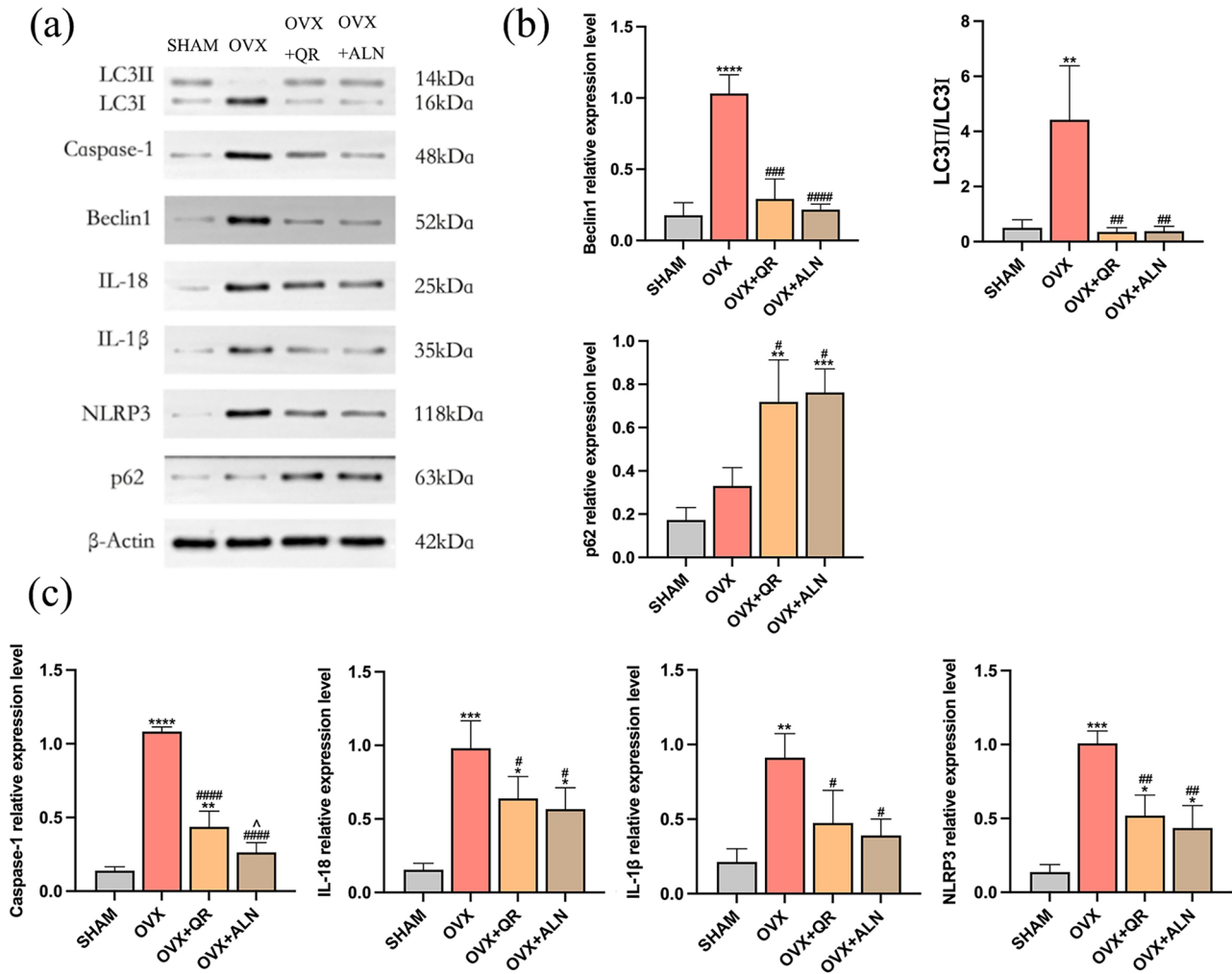


Figure 6. Effect of OVX and treatment using QR or ALN on the expression of NLRP3 pathway-related proteins as well as autophagy-related proteins. (a) Grayscale values of protein strips; (b) Western blotting showed the expression of Beclin1, p62, and LC3II/I ratio; and (c) Western blotting showed the expression of caspase-1, IL-18, IL-1 β , and NLRP3.

Data are expressed as mean (SD) of $n=6$ from three independent experiments.

* $P < 0.05$, ** $P < 0.01$, *** $P < 0.001$, **** $P < 0.0001$ compared with SHAM group.

$P < 0.05$, ## $P < 0.01$, ### $P < 0.001$, #### $P < 0.0001$ compared with OVX group.

^ $P < 0.05$ compared with OVX + QR group.

a decrease in osteocytes and bone volume. Compared to the OVX group, the rest of the treatment groups had relatively more intact bone structure, with slightly more bone trabeculae, lamellar and dense, reduced bone marrow cavity, significantly fewer fatty vacuoles and osteoclasts, more osteocytes, especially in the group that used M, CQ alone or in combination with QR. The number of blood vessels varied widely among the treatment groups, but it increased in all groups compared with the OVX group. The micro-CT results were further validated, indicating that QR treatment partially restored the lost bone mass in the alveolar bone of the OVX rats (see Figure 9).

Impact of QR on osteoclasts in the mandibular alveolar bone of OVX rats

TRAP staining of the mandibular alveolar bone tissues in each group showed that more obvious multinucleated, cytoplasmic red-stained osteoclasts in the alveolar bone tissues of the OVX group than in the SHAM group, spreading

over the surface of the bone trabeculae, and the number of TRAP-positive osteoclasts was significantly reduced in the remaining treatment groups, especially in the combined treatment group of QR with either CQ or M, in which the TRAP-positive osteoclasts stained very superficially, rarely in number, and were almost unable to be detected. These results further suggested that QR may inhibit the number of osteoclasts in the alveolar bone in the osteoporotic state to alleviate bone resorption, and that CQ or M may be able to enhance the ability of QR to inhibit osteoclasts (see Figure 10).

Discussion

Meta-analysis showed that significant bone loss was observed around dental implants placed in osteoporotic patients compared to the non-osteoporotic population, which is a big challenge for the long-term success of implant restorations.²⁴ Natural products are an excellent and reliable means of preventing OP, because they have fewer side

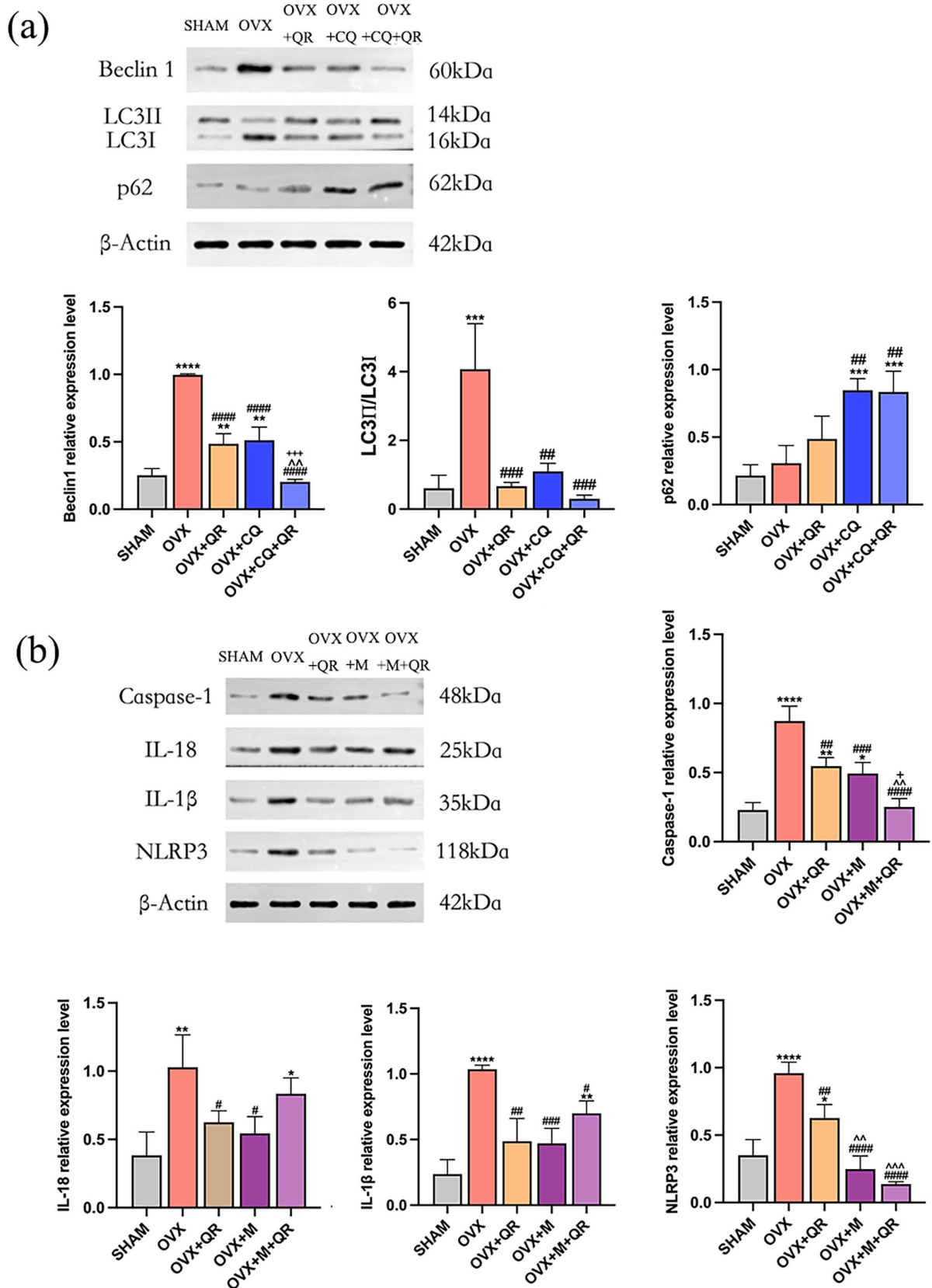


Figure 7. (a) Western blotting showed the effect of QR and CQ on the expression of autophagy-related proteins and (b) Western blotting showed the effect of QR and MCC950 on the expression of NLRP3 pathway-related proteins. Data are expressed as mean (SD) of $n=6$ from three independent experiments. * $P < 0.05$, ** $P < 0.01$, *** $P < 0.001$, **** $P < 0.0001$ compared with SHAM group. # $P < 0.05$, ## $P < 0.01$, ### $P < 0.001$, #### $P < 0.0001$ compared with OVX group. ^^ $P < 0.01$, ^^ $P < 0.001$ compared with OVX + QR group. + $P < 0.05$, +++ $P < 0.001$ compared with OVX + CQ group or OVX + M group.

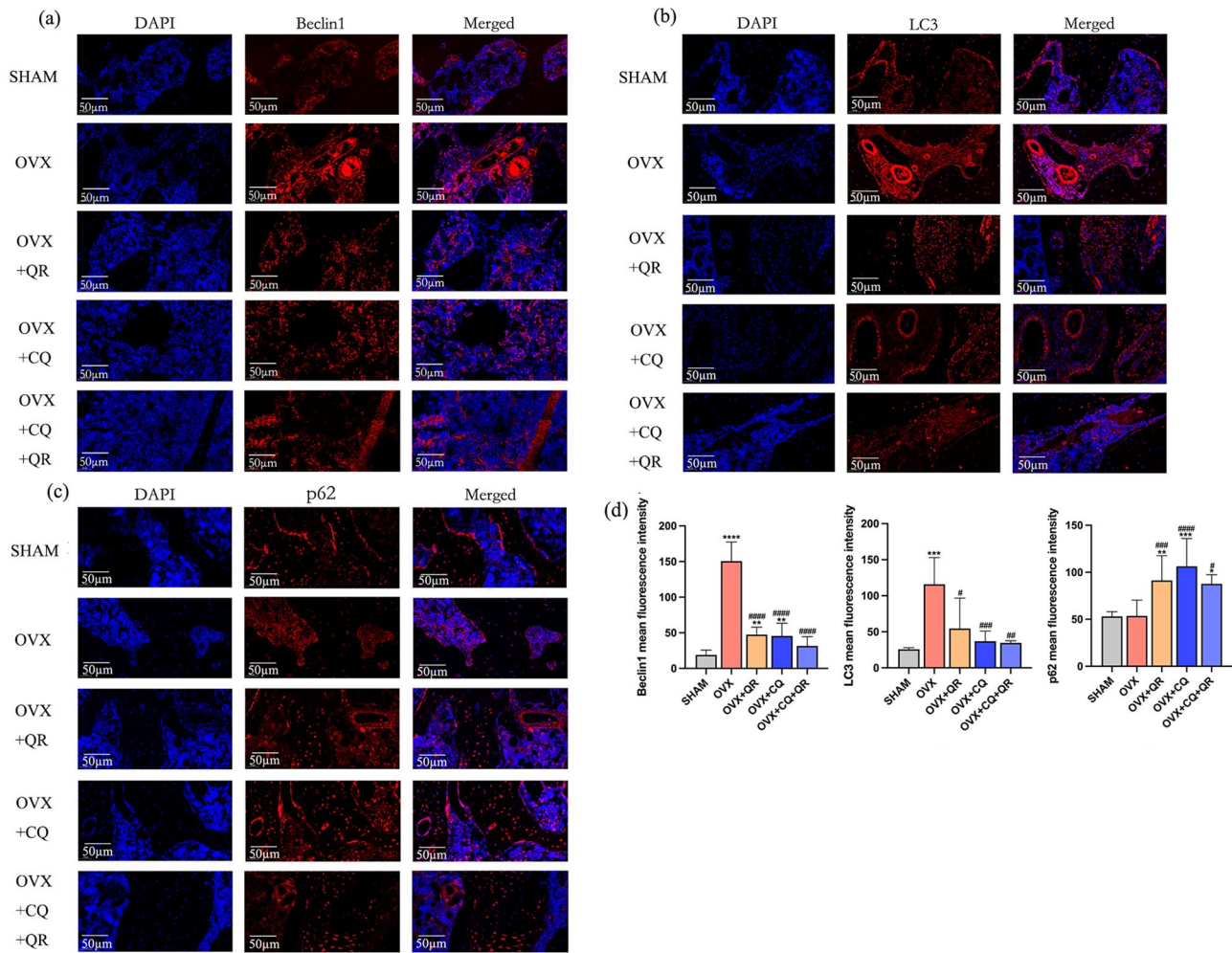


Figure 8. Expression of (a) Beclin1, (b) LC3, and (c) p62 in mandibular alveolar bone in rats detected by immunofluorescence staining (Magnification, $\times 200$; scale bar, 50 μm); and (d) quantification of the mean fluorescence intensity of Beclin1, LC3, and p62.

Data are expressed as mean (SD) of $n=5$ from five independent experiments.

DAPI: 4',6-diamidino-2-phenylindole.

* $P < 0.05$, ** $P < 0.01$, *** $P < 0.001$, **** $P < 0.0001$ compared with SHAM group.

$P < 0.05$, ## $P < 0.01$, ### $P < 0.001$, #### $P < 0.0001$ compared with OVX group.

effects, are less costly, and are more suitable for long-term applications. Natural QR is widely available in the daily intake of fruits, vegetables, tea, and wine, although the dietary intake of QR is only 3–40 mg per day, which is much lower than the recommended daily intake of 500–1000 mg from nutritional supplements.²⁵ QR has shown favorable anti-osteoporotic effects in a variety of OP models in rats and mice, including female rats and mice with OP due to bilateral OVX^{26–30} and various other types of OP: rats with glucocorticoid-induced osteoporosis (GIO) due to subcutaneous injection of methylprednisolone sodium succinate,³¹ rats with diabetic osteopenia due to intraperitoneal injection of streptozotocin,³² oral administration of nano-zinc oxide induced perturbation of bone turnover in male rats³³ and wasting OP due to immobilization of the hind limbs in mice.³⁴ Administration of QR significantly increased Tb. Th,^{26,29} Tb. N,^{26,29,31} BMD,^{26–29,32} and the content of the bone formation marker osteocalcin in the lumbar spine or femur of both rats and mice.^{31,32} QR at 50 mg/kg/day for 30 days decreased alkaline phosphatase (ALP) levels, acid

phosphatase (ACP) levels, as well as elevated serum Ca and P levels,³⁰ while a high dose of QR at 150 mg/kg resulted in a 22% increase in bone cortical thickness in addition to a more substantial improvement in bone trabecular microstructure.³¹ QR also significantly increased the maximum load of bone and improved the biomechanical properties of bone.^{26–28,31,32} As an antioxidant, QR reduces pro-inflammatory markers: tumor necrosis factor α (TNF- α), IL-6 and C-reactive protein (CRP) to mitigate inflammatory responses to prevent and treat bone loss.³³ However, QR does not appear to produce estrogenic activity through estrogen receptors and would not be a selective modulator of estrogen receptors *in vivo*.²⁹ Besides, QR increases the expression of the vascular endothelial growth factor (VEGF), angiogenin-1 (ANG-1), basic fibroblast growth factor (bFGF), and transforming growth factor- β (TGF- β), which contributes to angiogenesis, ultimately leading to the enhancement of bone regeneration.²¹ *In vitro* experiments demonstrated that QR promoted the expression of the antioxidant hormone stanniocalcin 1 (STC1) and reduced reactive oxygen species (ROS) production,

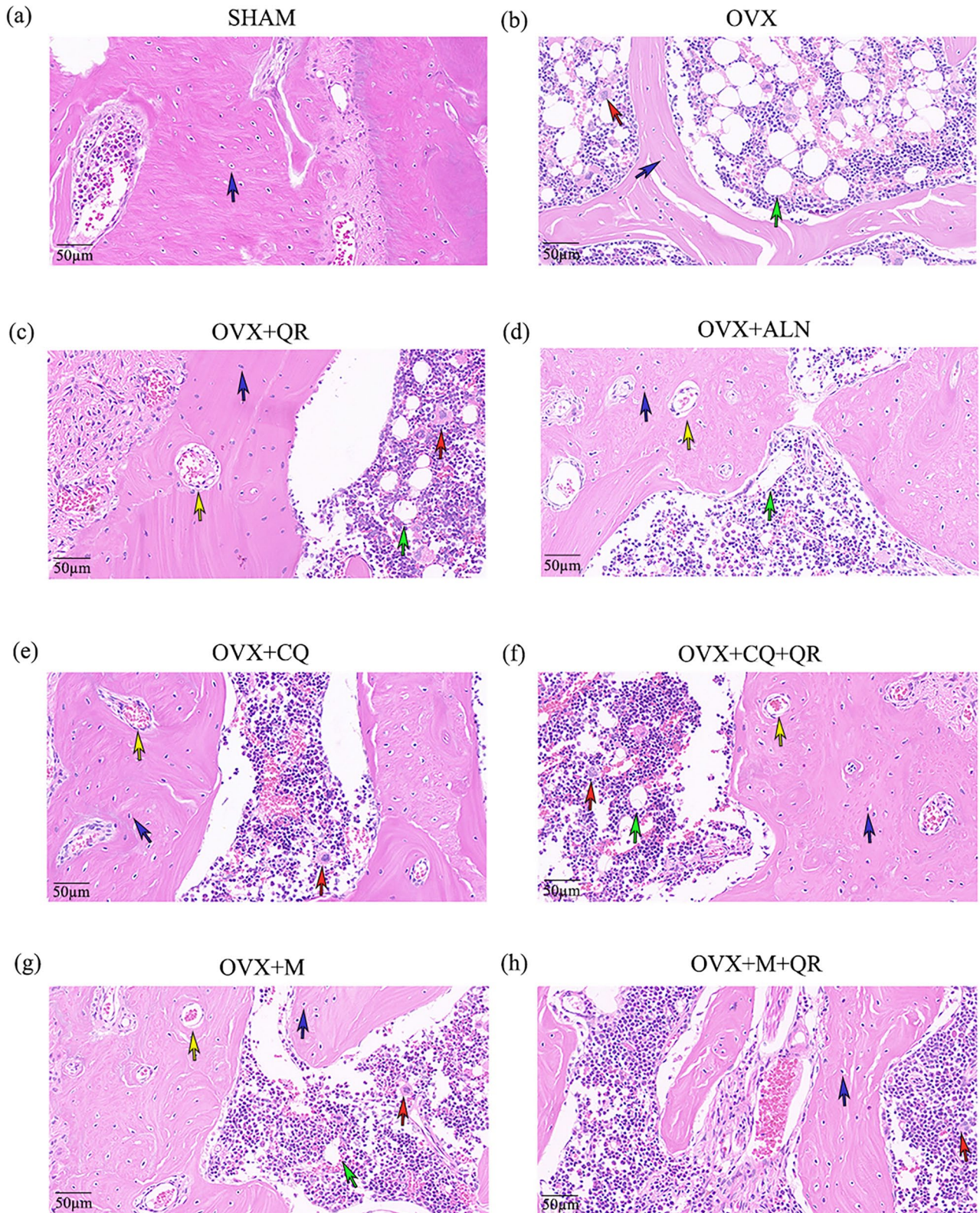


Figure 9. Hematoxylin-eosin (HE) staining showed the effects of QR on histopathological changes in the mandibular alveolar bone of OVX rats in (a) SHAM group, (b) OVX group, (c) OVX + QR group, (d) OVX + ALN group, (e) OVX + CQ group, (f) OVX + CQ + QR group, (g) OVX + M group, and (h) OVX + M + QR group (magnification, $\times 200$; scale bar, 50 μm). Sample size $n=5$. Blue arrows: osteocytes; Red arrows: osteoclasts; Green arrows: vacuolated fat cells; Yellow arrows: blood vessels.

dose-dependently inhibiting RANKL-induced osteoclast differentiation and expression of related genes.^{29,34} QR also inhibited lipopolysaccharides (LPS)-induced macrophage

inflammation and oxidative stress through anti-inflammation and ROS scavenging.³⁵ QR significantly restored mRNA expression of osteoblast-related genes inhibited by LPS in

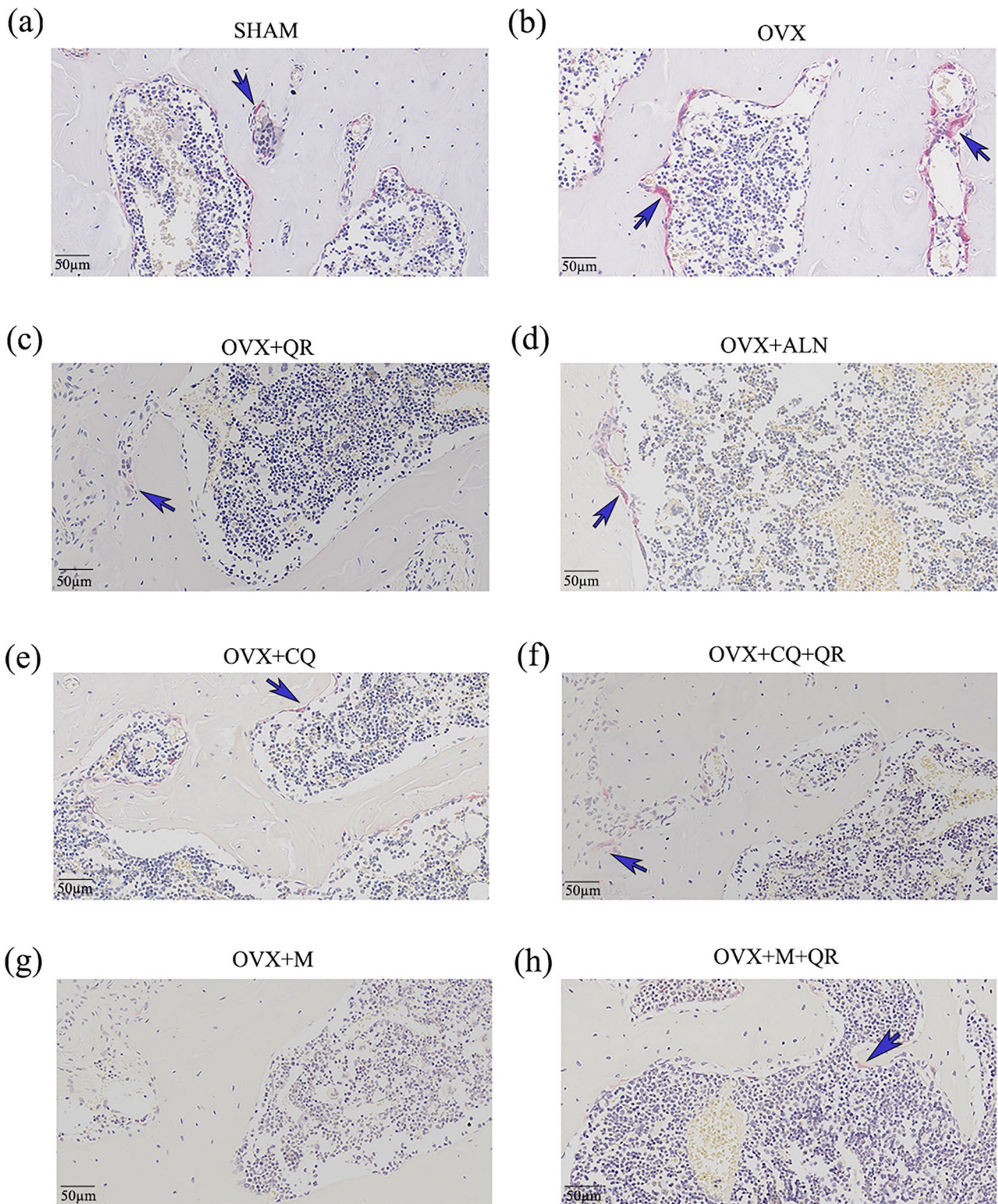


Figure 10. Anti-tartrate acid phosphatase (TRAP) staining showed the impact of QR on osteoclasts in the mandibular alveolar bone of OVX rats in (a) SHAM group, (b) OVX group, (c) OVX + QR group, (d) OVX + ALN group, (e) OVX + CQ group, (f) OVX + CQ + QR group, (g) OVX + M group, and (h) OVX + M + QR group (magnification, $\times 200$; scale bar, 50 μm). Sample size $n=5$. Blue arrow: TRAP-positive osteoclasts.

a dose-dependent manner via mitogen-activated protein kinase (MAPK) signaling, as well as osterix protein expression in mouse embryo osteoblast precursor cells (MC3 T3-E1), reversing the inhibition of osteoblast differentiation by

LPS.³⁶ For mesenchymal stem cells (MSCs), QR promotes osteogenic differentiation and inhibits adipogenic differentiation of murine bone marrow stem cells (mBMSCs) through activation of the MAPK/SIRT1 signaling pathway.³⁷ QR

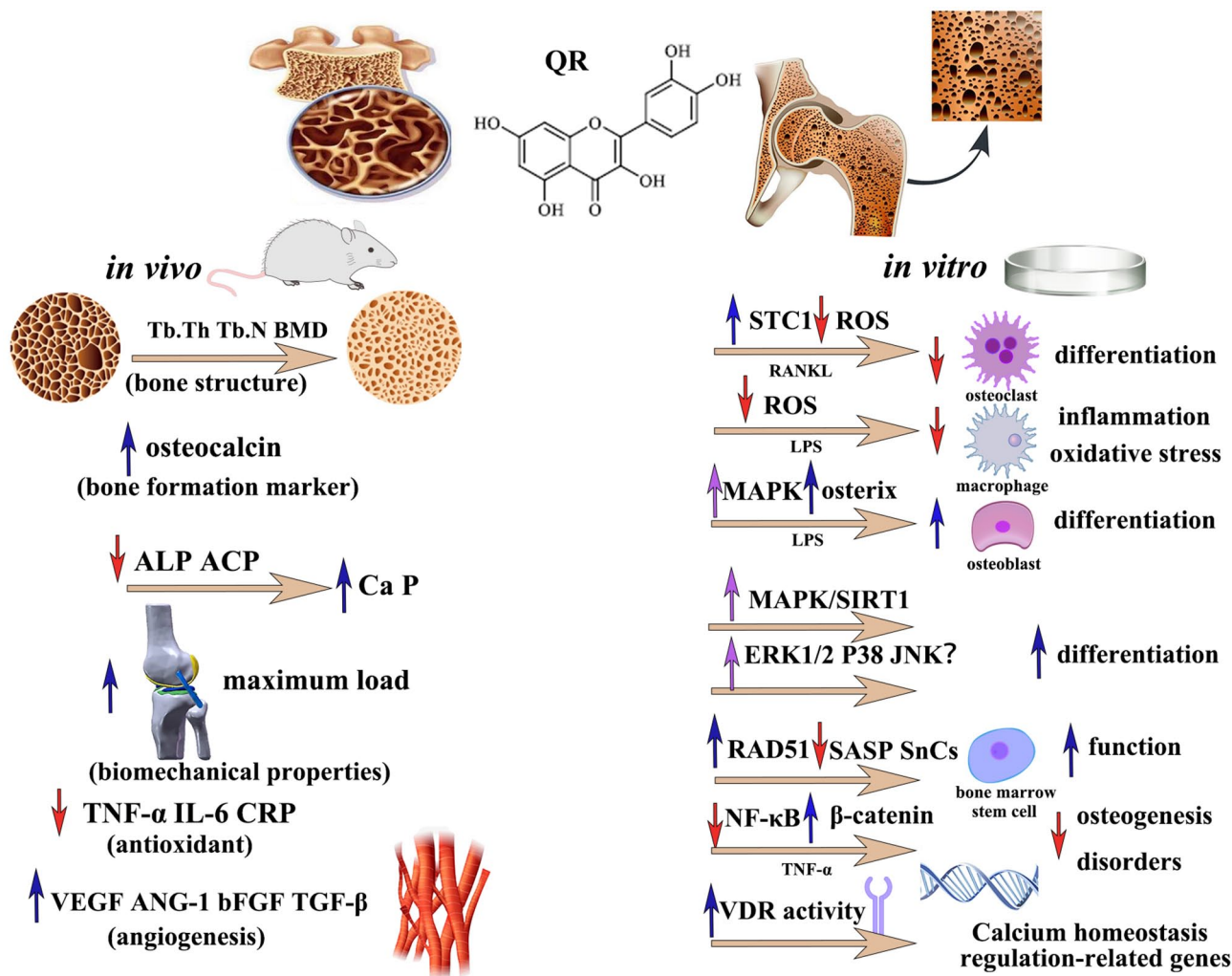


Figure 11. A schematic representation of the bone protective mechanism of quercetin in OP.

Blue arrow: increase; red arrow: decrease; purple arrow: activate.

ALP: alkaline phosphatase; ACP: acid phosphatase; TNF- α : tumor necrosis factor α ; IL-6: interleukin-6; CRP: C-reactive protein; VEGF: vascular endothelial growth factor; ANG-1: angiogenin-1; bFGF: basic fibroblast growth factor; TGF- β : transforming growth factor- β ; STC1: antioxidant hormone stanniocalcin 1; ROS: reactive oxygen species; RANKL: receptor activator of nuclear factor- κ B ligand; LPS: lipopolysaccharides; MAPK: mitogen-activated protein kinase; ERK1/2: extracellular regulated protein kinases; JNK: c-Jun N-terminal kinase; SASP: senescence-associated secretory phenotype; SnCs: senescent cells; NF- κ B: nuclear factor-kappa B; TNF- α : tumor necrosis factor- α ; VDR: vitamin D receptor.

can also promote mBMSCs differentiation by activating the extracellular regulated protein kinases (ERK1/2) and c-Jun N-terminal kinase (JNK) signaling pathway to regulate the expression of the TGF- β 1, the bone morphogenetic protein-2 (BMP-2), and the core-binding factor (CBF α 1),³⁸ but another study has reported that QR can activate the ERK and p38 signaling pathways but not the JNK signaling pathway.³⁹ QR also upregulates the DNA repair-related protein RAD51, attenuates the senescence-associated secretory phenotype (SASP), reduces the accumulation of senescent cells (SnCs), rescues BMSCs from failure, and restores its function.⁴⁰ In addition, QR inhibited NF- κ B activation and upregulated β -catenin, significantly suppressing TNF- α -induced BMSC osteogenesis disorders.²⁷ Moreover, it has been reported that QR, as a vitamin D receptor (VDR) activator, enhances VDR activity by altering the recruitment of cofactors, which modulates the expression of genes involved in calcium homeostasis.⁴¹ Figure 11 provides a simplified schematic demonstration of the bone protective mechanism of QR in

OP. Previous studies have mostly focused on the effects of QR on the long bones, but few studies have targeted the alveolar bone. The recent study combined high-dose ALN (5 g/kg/day) with low-dose QR (15 mg/kg/day), and using ELISA, stereological tests, RT-PCR, and immunofluorescence found that the combination of QR and ALN improved the total number of osteoblasts and bone remodeling indexes in the femur of OVX rats better compared with ALN alone with significant downregulation of autophagy markers and apoptosis-associated genes, hypothesizing that the combination of these two may be an effective therapeutic strategy for the treatment of OP in postmenopausal women.⁴² Our study simulated the daily recommended intake of QR supplements, as well as the frequency and dose of clinical ALN intake, with the addition of autophagy and NLRP3 pathway inhibitor treatment groups. Our study aimed to assess more intuitively and systematically whether QR alone as a dietary supplement could achieve similar therapeutic effects of ALN in the OVX-induced mandibular OP in female rats from the

perspectives of autophagy and the NLRP pathway by micro-CT, western blotting, and other methods.

Ovarian hormones have been shown to play a critical role in metabolism, appetite, and body weight regulation in female animals, and reduced hormone levels after OVX increase food intake and body weight, leading to obesity in experimental animals.⁴³ Treatment with QR, ALN, CQ, and MCC950 reversed the changes in body weight in the OVX rats; and although body weight was still higher in the treated group than in the SHAM group, this was not equivalent to changes in bone mass but was still a positive development in terms of weight control. Both QR and ALN increased BV/TV, Tb. N, Tb. Th, and BMD, and decreased Tb. Sp in OVX rats. Trabecular bone-related index reflects changes in bone microstructure and are important indicators for evaluating OP, while BMD is the main indicator for evaluating the effect of OP treatment.⁴⁴ Our results show that QR can improve bone microstructure, enhance bone quality, effectively increase BMD in PMOP rats, and treat PMOP from a structural perspective, achieving therapeutic effects similar to those of ALN.

The International Osteoporosis Foundation (IOF) recommends the use of PINP and CTX-1 in OP clinical trials as preferred markers for clinical assessment of bone turnover.⁴⁵ Although not used for the diagnosis of OP, they are valuable for patient assessment and improve the ability to identify certain secondary causes of OP, and are also effective in monitoring treatment adherence.⁴⁶ Therefore, in this study, PINP and CTX-1 were selected as indicators to evaluate the effectiveness of using QR and ALN in the management of PMOP. PINP is derived from the post-translational shearing of type 1 procollagen and is expressed mainly during the proliferative phase of osteoblasts, whereas CTX-1 is a degradation product of type 1 collagen and reflects the active state of osteoclasts. In this study, the serological bone turnover indices (CTX-1 and PINP) were high in rats in the untreated OVX group, indicating a markedly progressive and abnormal bone remodeling process and bone resorption activity. High bone turnover is typical in most postmenopausal women, with bone mass decreasing dramatically at this stage.⁴⁷ However, QR and ALN decreased PINP, and CTX-1. The combination of QR and MCC950 or CQ resulted in an even more significant reduction in PINP and CTX-1, similar to the results of previous studies,⁴⁸ suggesting that QR may play a dual role in inhibiting bone resorption and promoting bone formation. However, the exact underlying mechanisms require further investigation.

NLRP3 activation during osteoclast activation can lead to the development of inflammatory diseases. NLRP3 functions as an intracellular multiprotein complex that triggers cell death in response to the combined action of pathogens (PAMPs) and damage-associated molecular patterns (DAMPs). Recognition of endogenous and exogenous factors leads to the formation of the NLRP3/apoptosis-associated speck-like protein containing a CARD (ASC), ASC/pro-caspase-1 inflammatory complex, which activates caspase-1 and acts on the processing precursors IL-1 β and IL-18, resulting in the release of mature cytokines and triggering an inflammatory response.⁴⁹ IL-1 β is one of the leading members of the IL-1 family, which plays an essential role in bone loss following estrogen deficiency,⁵⁰ and is not only a

potent stimulator of bone resorption but also a potent inhibitor of osteogenesis. IL-18 and IL-1 β are closely related, share a similar three-dimensional (3D) structure, and promote osteoclast differentiation through multiple pathways. IL-1 β and IL-18 are involved in and prolonging the OP inflammatory response.⁸ MCC950 is a potent and specific NLRP3 inflammasome inhibitor. *In vivo* experiments showed that NLRP3 knockdown and supplementation with MCC950 significantly reduced age-related alveolar bone loss in aged mice, resulting in higher BMD and bone mass per unit tissue.⁵¹ *In vitro* experiments showed that MCC950 indirectly regulates osteoclastogenesis by inhibiting IL-1 β secretion from specific sites of macrophages and/or PMNs, and also directly controls osteoclast differentiation independent of IL-1 β maturation by inhibiting RANKL-induced caspase-1 activation.⁸ In line with the findings, QR was comparable to ALN and MCC950 in reducing inflammatory mediators, and the combination of MCC950 and QR resulted in a more effective reduction of caspase-1.

Autophagy plays a protective role in organisms and is primarily responsible for eliminating damaged or excess organelles to maintain normal metabolism. Abnormal autophagy disrupts bone homeostasis, and proper regulation of autophagy is essential for maintaining normal cellular metabolism and function.⁵² p62, also known as Sequestosome1, is a marker protein that reflects autophagic activity.⁵³ p62/SQSTM1 is an autophagic selective substrate that is severely consumed when autophagic vesicles bind to lysosomes to degrade their contents⁵⁴ and act as an autophagic adaptor. The microtubule-associated protein LC3 regulates autophagosome formation. Under normal conditions, LC3 exists as LC3I, and when autophagy is activated, a conversion of LC3I to LC3II can be observed,⁵⁵ with a gradual increase in LC3II/I.⁵⁶ Beclin1 is another essential protein in autophagosome formation,⁵⁷ and it is not only a component of the PI3K complex but also a principal autophagy regulator.⁵⁸ Thus, during autophagy activation, Beclin1 and LC3II are upregulated, while p62 decreases; conversely, inhibition of autophagy leads to a decrease in Beclin1 and LC3II and an accumulation of p62. CQ is a lysosomal inhibitor that inactivates acid hydrolases in lysosomes by disrupting the acidic environment within lysosomes, autophagosome degradation fails, and LC3 accumulates. In addition, CQ inhibits the fusion of LC3-positive autophagosomes with lysosomes, thereby affecting lysosomal function and preventing the autophagic process.⁵⁹ Beclin-1 induces RANKL-mediated Atg activation and osteoclast differentiation through ubiquitination during the differentiation of osteoclast progenitor cells into osteoclasts.⁶⁰ Absence of LC3II leads to the formation of disordered actin structures that severely impair the migratory ability of osteoclasts.⁶¹ Enhanced osteoclast-mediated bone resorption is critical in the early stages of PMOP and rapid glucocorticoid-induced bone loss, suggesting that inhibition of osteoclastic autophagy activity may be potent in reversing bone loss. Consistent with previous studies,⁴² western blot and immunofluorescence results revealed a decrease in Beclin1, LC3II/I, and an accumulation of p62, and the effect of QR alone was comparable to that of ALN. HE and TRAP staining also showed that treatment with QR resulted in a tidier arrangement of bone trabeculae, a marked

decrease in fat vacuoles and osteoclasts, and an increase in osteocytes. The rat skeletal pathology was repaired, and the bone metabolism remained balanced. In terms of bone microenvironment alterations, both QR and ALN treatments achieved good results, with no significant differences. However, there was no discernible difference in the protein expression of p62 between the QR and OVX groups, probably because genes related to autophagy can be induced by various triggers of cellular stress, such as oxidative stress, estrogen, and endoplasmic reticulum contingency. It has been reported that the loss of lysosomal function associated with CQ is exacerbated by concurrent treatment with QR.⁶² In our experiments, the inhibitory effect of QR on autophagy was comparable to that of CQ, and in combination, it significantly reduced the expression of PINP, and Beclin1, and was more effective in the inhibition of osteoclasts, suggesting that CQ and QR may have a synergistic effect in the treatment of OP, and the specific mechanism remains to be further explored.

This study has some limitations. Due to the limited sample size, the comparison of the effect of QR at different doses and the detection of PMOP markers such as alkaline phosphatase were not performed. The therapeutic effect of QR on PMOP was confirmed only from a structural aspect, and no analysis of bone mechanical properties was performed. Further studies are required to determine whether QR can improve bone function.

In conclusion, QR reduces estrogen-deficiency-induced bone loss and protects bone mass in OVX rats with effects comparable to those of ALN, possibly by inhibiting NLRP3-mediated production of inflammatory factors and suppressing osteoclast autophagy. Our findings confirm the potential of QR as a natural product to prevent and treat bone loss, with a view to improving the long-term stability of implant prostheses in patients with PMOP through the daily administration of QR as a nutraceutical.

AUTHORS' CONTRIBUTIONS

JL, YX, and C-WH designed and conceived the experiments, and confirmed the authenticity of all original data. YX, C-WH, CS, and LP performed the experiments. YX and C-WH drafted the article. YX, C-WH, Y-TC, CS, and LP analyzed the experimental data. JL, YX, C-WH, Y-TC, and WH reviewed and revised the article. JL contributed reagents/materials/funds. All authors read and approved the final article.

DECLARATION OF CONFLICTING INTERESTS

The author(s) declared no potential conflicts of interest with respect to the research, authorship, and/or publication of this article.

FUNDING

The author(s) disclosed receipt of the following financial support for the research, authorship, and/or publication of this article: This research was funded by the National Natural Science Foundation of China (grant no. 82060207, 82260198); Natural Science Foundation Project of Guizhou Province: Key Basic Science Project Contract (grant no. ZK[2023]037); Guizhou Health and Health Committee Science and Technology Fund Program (grant no. gzwkj2023-439).

ORCID IDS

Yue Xiong  <https://orcid.org/0000-0002-7926-9939>

Jian Liao  <https://orcid.org/0000-0003-3519-4485>

REFERENCES

- Ma M, Chen X, Lu L, Yuan F, Zeng W, Luo S, Yin F, Cai J. Identification of crucial genes related to postmenopausal osteoporosis using gene expression profiling. *Aging Clin Exp Res* 2016;**28**:1067–74
- Yang C, Ren J, Li B, Jin C, Ma C, Cheng C, Sun Y, Shi X. Identification of gene biomarkers in patients with postmenopausal osteoporosis. *Mol Med Rep* 2019;**19**:1065–73
- Black DM, Rosen CJ. Clinical practice. Postmenopausal osteoporosis. *N Engl J Med* 2016;**374**:254–62
- Taniyama T, Saruta J, Mohammadzadeh Rezaei N, Nakhaei K, Ghassemi A, Hirota M, Okubo T, Ikeda T, Sugita Y, Hasegawa M, Ogawa T. UV-photofunctionalization of titanium promotes mechanical anchorage in a rat osteoporosis model. *Int J Mol Sci* 2020;**21**:1235
- DeSelm CJ, Miller BC, Zou W, Beatty WL, van Meel E, Takahata Y, Klumperman J, Tooze SA, Teitelbaum SL, Virgin HW. Autophagy proteins regulate the secretory component of osteoclastic bone resorption. *Dev Cell* 2011;**21**:966–74
- Wilhelm T, Richly H. Autophagy during ageing – from Dr Jekyll to Mr Hyde. *FEBS J* 2018;**285**:2367–76
- He W, Zheng Y, Feng Q, Elkhooly TA, Liu X, Yang X, Wang Y, Xie Y. Silver nanoparticles stimulate osteogenesis of human mesenchymal stem cells through activation of autophagy. *Nanomedicine* 2020;**15**:337–53
- Jiang N, An J, Yang K, Liu J, Guan C, Ma C, Tang X. NLRP3 inflammation: a new target for prevention and control of osteoporosis? *Front Endocrinol* 2021;**12**:752546
- Li X, Xu J, Dai B, Wang X, Guo Q, Qin L. Targeting autophagy in osteoporosis: from pathophysiology to potential therapy. *Ageing Res Rev* 2020;**62**:101098
- Briot K, Geusens P, Em Bultink I, Lems WF, Roux C. Inflammatory diseases and bone fragility. *Osteoporos Int* 2017;**28**:3301–14
- Mbalaviele G, Novack DV, Schett G, Teitelbaum SL. Inflammatory osteolysis: a conspiracy against bone. *J Clin Invest* 2017;**127**:2030–9
- Clarke AJ, Simon AK. Autophagy in the renewal, differentiation and homeostasis of immune cells. *Nat Rev Immunol* 2019;**19**:170–83
- Chen LR, Ko NY, Chen KH. Medical treatment for osteoporosis: from molecular to clinical opinions. *Int J Mol Sci* 2019;**20**:2213
- Faienza MF, Chiarito M, D'amato G, Colaianni G, Colucci S, Grano M, Brunetti G. Monoclonal antibodies for treating osteoporosis. *Expert Opin Biol Ther* 2018;**18**:149–57
- Kling JM, Clarke BL, Sandhu NP. Osteoporosis prevention, screening, and treatment: a review. *J Womens Health* 2014;**23**:563–72
- Minisola S, Vargas AP, Letizia Mauro G, Bonet Madurga F, Adami G, Black DM, Qizilbash N, Blanch-Rubió J. A prospective open-label observational study of a buffered soluble 70 mg alendronate effervescent tablet on upper gastrointestinal safety and medication errors: the gastroPASS study. *JBMR Plus* 2021;**5**:e10510
- Qi W, Qi W, Xiong D, Long M. Quercetin: its antioxidant mechanism, antibacterial properties and potential application in prevention and control of toxipathy. *Molecules* 2022;**27**:6545
- Jana N, Břetislav G, Pavel S, Pavla U. Potential of the flavonoid quercetin to prevent and treat cancer – current status of research. *Klin Onkol* 2018;**31**:184–90
- Castelo-Branco C, Soveral I. Phytoestrogens and bone health at different reproductive stages. *Gynecol Endocrinol* 2013;**29**:735–43
- Srivastava S, Bankar R, Roy P. Assessment of the role of flavonoids for inducing osteoblast differentiation in isolated mouse bone marrow derived mesenchymal stem cells. *Phytomedicine* 2013;**20**:683–90
- Wong SK, Chin KY, Ima-Nirwana S. Quercetin as an agent for protecting the bone: a review of the current evidence. *Int J Mol Sci* 2020;**21**:6448
- Abdulkadir A, Mbajorgu EF, Nyirenda T. Effects of concurrent chloroquine and ethanol administration on the rat kidney morphology. *Pan Afr Med J* 2018;**29**:49
- Zhang C, Huang Y, Ouyang F, Su M, Li W, Chen J, Xiao H, Zhou X, Liu B. Extracellular vesicles derived from mesenchymal stem cells alleviate

- neuroinflammation and mechanical allodynia in interstitial cystitis rats by inhibiting NLRP3 inflammasome activation. *J Neuroinflammation* 2022;19(1):80
24. Lemos CAA, de Oliveira AS, Faé DS, Oliveira HFFE, Del Rei Dal-tro Rosa CD, Bento VAA, Verri FR, Pellizzer EP. Do dental implants placed in patients with osteoporosis have higher risks of failure and marginal bone loss compared to those in healthy patients? A systematic review with meta-analysis. *Clin Oral Investig* 2023;27:2483–93
 25. Andres S, Pevny S, Ziegenhagen R, Bakhiya N, Schäfer B, Hirsch-Ernst KI, Lampen A. Safety aspects of the use of quercetin as a dietary supplement. *Mol Nutr Food Res*. Epub ahead of print 19 December 2017. DOI: 10.1002/mnfr.201700447
 26. Siddiqui JA, Sharan K, Swarnkar G, Rawat P, Kumar M, Manickavasagam L, Maurya R, Pierroz D, Chattopadhyay N. Quercetin-6-C- β -D-glucopyranoside isolated from *Ulmus wallichiana* planchon is more potent than quercetin in inhibiting osteoclastogenesis and mitigating ovariectomy-induced bone loss in rats. *Menopause* 2011;18:198–207
 27. Yuan Z, Min J, Zhao Y, Cheng Q, Wang K, Lin S, Luo J, Liu H. Quercetin rescued TNF- α -induced impairments in bone marrow-derived mesenchymal stem cell osteogenesis and improved osteoporosis in rats. *Am J Transl Res* 2018;10:4313–21
 28. Xing LZ, Ni HJ, Wang YL. Quercitrin attenuates osteoporosis in ovariectomized rats by regulating mitogen-activated protein kinase (MAPK) signaling pathways. *Biomed Pharmacother* 2017;89:1136–41
 29. Tsuji M, Yamamoto H, Sato T, Mizuha Y, Kawai Y, Taketani Y, Kato S, Terao J, Inakuma T, Takeda E. Dietary quercetin inhibits bone loss without effect on the uterus in ovariectomized mice. *J Bone Miner Metab* 2009;27:673–81
 30. Abd El-Fattah AI, Fathy MM, Ali ZY, El-Garawany AEA, Mohamed EK. Enhanced therapeutic benefit of quercetin-loaded phytosome nanoparticles in ovariectomized rats. *Chem Biol Interact* 2017;271:30–8
 31. Derakhshanian H, Djalali M, Djazayeri A, Nourijelyani K, Ghadbeigi S, Pishva H, Saedisomeolia A, Bahremand A, Dehpour AR. Quercetin prevents experimental glucocorticoid-induced osteoporosis: a comparative study with alendronate. *Can J Physiol Pharmacol* 2013;91:380–5
 32. Liang W, Luo Z, Ge S, Li M, Du J, Yang M, Yan M, Ye Z, Luo Z. Oral administration of quercetin inhibits bone loss in rat model of diabetic osteopenia. *Eur J Pharmacol* 2011;670:317–24
 33. Abdelkarem HM, Fadda LM, Kaml OR. Alleviation of bone markers in rats induced nano-zinc oxide by quercetin and α -lipoic acid. *Toxicol Mech Methods* 2016;26:692–9
 34. Niu YB, Yang YY, Xiao X, Sun Y, Zhou YM, Zhang YH, Dong D, Li CR, Wu XL, Li YH, Mei QB. Quercetin prevents bone loss in hindlimb suspension mice via stanniocalcin 1-mediated inhibition of osteoclastogenesis. *Acta Pharmacol Sin* 2020;41:1476–86
 35. Tang J, Diao P, Shu X, Li L, Xiong L. Quercetin and quercitrin attenuates the inflammatory response and oxidative stress in LPS-induced RAW264.7 cells: in vitro assessment and a theoretical model. *Biomed Res Int* 2019;2019:7039802
 36. Wang XC, Zhao NJ, Guo C, Chen JT, Song JL, Gao L. Quercetin reversed lipopolysaccharide-induced inhibition of osteoblast differentiation through the mitogen-activated protein kinase pathway in MC3T3-E1 cells. *Mol Med Rep* 2014;10:3320–6
 37. Wang N, Wang L, Yang J, Wang Z, Cheng L. Quercetin promotes osteogenic differentiation and antioxidant responses of mouse bone mesenchymal stem cells through activation of the AMPK/SIRT1 signaling pathway. *Phytother Res* 2021;35:1–12
 38. Li Y, Wang J, Chen G, Feng S, Wang P, Zhu X, Zhang R. Quercetin promotes the osteogenic differentiation of rat mesenchymal stem cells via mitogen-activated protein kinase signaling. *Exp Ther Med* 2015;9:2072–80
 39. Zhou C, Lin Y. Osteogenic differentiation of adipose-derived stem cells promoted by quercetin. *Cell Prolif* 2014;47:124–32
 40. Wang Y, Che L, Chen X, He Z, Song D, Yuan Y, Liu C. Repurpose dasatinib and quercetin: targeting senescent cells ameliorates postmenopausal osteoporosis and rejuvenates bone regeneration. *Bioact Mater* 2023;25:13–28
 41. Inoue J, Choi JM, Yoshidomi T, Yashiro T, Sato R. Quercetin enhances VDR activity, leading to stimulation of its target gene expression in Caco-2 cells. *J Nutr Sci Vitaminol* 2010;56:326–30
 42. Mousavi S, Vakili S, Zal F, Savardashtaki A, Jafarinia M, Sabetian S, Razmjou D, Veisi A, Azadbakht O, Sabaghan M, Behrouj H. Quercetin potentiates the anti-osteoporotic effects of alendronate through modulation of autophagy and apoptosis mechanisms in ovariectomy-induced bone loss rat model. *Mol Biol Rep* 2023;50:3693–703
 43. Iwasa T, Matsuzaki T, Yano K, Irahara M. The effects of ovariectomy and lifelong high-fat diet consumption on body weight, appetite, and lifespan in female rats. *Horm Behav* 2018;97:25–30
 44. Khairallah P, Nickolas TL. Management of osteoporosis in CKD. *Clin J Am Soc Nephrol* 2018;13:962–9
 45. Lorentzon M, Branco J, Brandi ML, Bruyère O, Chapurlat R, Cooper C, Cortet B, Diez-Perez A, Ferrari S, Gasparik A, Herrmann M, Jorgensen NR, Kanis J, Kaufman JM, Laslop A, Locquet M, Matijevic R, McCloskey E, Minisola S, Pikner R, Reginster JY, Rizzoli R, Szulc P, Vlasovska M, Cavalier E. Algorithm for the use of biochemical markers of bone turnover in the diagnosis, assessment and follow-up of treatment for osteoporosis. *Adv Ther* 2019;36:2811–24
 46. Kanis JA, Cooper C, Rizzoli R, Reginster JY; Scientific Advisory Board of the European Society for Clinical and Economic Aspects of Osteoporosis and Osteoarthritis (ESCEO) and the Committees of Scientific Advisors and National Societies of the International Osteoporosis Foundation (IOF). Executive summary of the European guidance for the diagnosis and management of osteoporosis in postmenopausal women. *Calcif Tissue Int* 2019;104:235–8
 47. Cavalier E, Bergmann P, Bruyère O, Delanaye P, Durnez A, Devogelaer JP, Ferrari SL, Gielen E, Goemaere S, Kaufman JM, Toukap AN, Reginster JY, Rousseau AF, Rozenberg S, Scheen AJ, Body JJ. The role of biochemical of bone turnover markers in osteoporosis and metabolic bone disease: a consensus paper of the Belgian Bone Club. *Osteoporos Int* 2016;27:2181–95
 48. Yuan YF, Wang S, Zhou H, Tang BB, Liu Y, Huang H, He CJ, Chen TP, Fang MH, Liang BC, Mao YD, Qie FQ, Liu K, Shi XL. Exploratory study of sea buckthorn enhancing QiangGuYin efficacy by inhibiting CKIP-1 and Notum activating the Wnt/ β -catenin signaling pathway and analysis of active ingredients by molecular docking. *Front Pharmacol* 2022;13:994995
 49. Kelley N, Jeltema D, Duan Y, He Y. The NLRP3 inflammasome: an overview of mechanisms of activation and regulation. *Int J Mol Sci* 2019;20:3328
 50. Khosla S. Pathogenesis of age-related bone loss in humans. *J Gerontol A Biol Sci Med Sci* 2013;68:1226–35
 51. Zang Y, Song JH, Oh SH, Kim JW, Lee MN, Piao X, Yang JW, Kim OS, Kim TS, Kim SH, Koh JT. Targeting NLRP3 inflammasome reduces age-related experimental alveolar bone loss. *J Dent Res* 2020;99:1287–95
 52. Dikic I, Elazar Z. Mechanism and medical implications of mammalian autophagy. *Nat Rev Mol Cell Biol* 2018;19:349–64
 53. Nogalska A, Terracciano C, D'Agostino C, King Engel W, Askanas V. p62/SQSTM1 is overexpressed and prominently accumulated in inclusions of sporadic inclusion-body myositis muscle fibers, and can help differentiating it from polymyositis and dermatomyositis. *Acta Neuropathol* 2009;118:407–13
 54. Sánchez-Martín P, Saito T, Komatsu M. p62/SQSTM1: “Jack of all trades” in health and cancer. *FEBS J* 2019;286:8–23
 55. Chen C, Kapoor A, Iozzo RV. Methods for monitoring matrix-induced autophagy. *Methods Mol Biol* 2019;1952:157–91
 56. Tanida I, Yamaji T, Ueno T, Ishiura S, Kominami E, Hanada K. Consideration about negative controls for LC3 and expression vectors for four colored fluorescent protein-LC3 negative controls. *Autophagy* 2008;4:131–4
 57. Galluzzi L, Baehrecke EH, Ballabio A, Boya P, Bravo-San Pedro JM, Cecconi F, Choi AM, Chu CT, Codogno P, Colombo MI, Cuervo AM, Debnath J, Deretic V, Dikic I, Eskelinen EL, Fimia GM, Fulda S, Gewirtz DA, Green DR, Hansen M, Harper JW, Jäättelä M, Johansen T, Juhasz G, Kimmelman AC, Kraft C, Ktistakis NT, Kumar S, Levine B, Lopez-Otin C, Madeo F, Martens S, Martinez J, Melendez A, Mizushima N, Münz C, Murphy LO, Penninger JM, Piacentini M, Reggiori F, Rubinsztein DC, Ryan KM, Santambrogio L, Scorrano L, Simon AK, Simon HU, Simonsen A, Tavernarakis N, Tooze SA, Yoshimori T, Yuan J, Yue Z, Zhong Q, Kroemer G. Molecular definitions of autophagy and related processes. *EMBO J* 2017;36:1811–36

58. Simon HU, Friis R, Tait SW, Ryan KM. Retrograde signaling from autophagy modulates stress responses. *Sci Signal* 2017;**10**:eaag2791
59. Wang S, Yang Y, Luo D, Zhai L, Bai Y, Wei W, Sun Q, Jia L. Bisphenol A increases TLR4-mediated inflammatory response by up-regulation of autophagy-related protein in lung of adolescent mice. *Chemosphere* 2021;**268**:128837
60. Arai A, Kim S, Goldshteyn V, Kim T, Park NH, Wang CY, Kim RH. Beclin1 modulates bone homeostasis by regulating osteoclast and chondrocyte differentiation. *J Bone Miner Res* 2019;**34**:1753–66
61. Zhang Y, Cui Y, Wang L, Han J. Autophagy promotes osteoclast podosome disassembly and cell motility through the interaction of kindlin3 with LC3. *Cell Signal* 2020;**67**:109505
62. Jang E, Kim IY, Kim H, Lee DM, Seo DY, Lee JA, Choi KS, Kim E. Quercetin and chloroquine synergistically kill glioma cells by inducing organelle stress and disrupting Ca²⁺ homeostasis. *Biochem Pharmacol* 2020;**178**:114098

(Received April 25, 2023, Accepted August 29, 2023)